Lanthanum-Substituted Nickel-Zinc used as Fillers for Composites

M. Šoka[1], M. Ušáková[1], R. Dosoudil[1], V. Jančárik, J. Škriniarová[2] and E. Ušák[1]

[1]Institute of Electrical Engineering, Faculty of Electrical Engineering and Information Technology, Slovak University of Technology in Bratislava, Ilkovičova 3, 841 04 Bratislava, Slovakia
[2]Institute of Informatics, Slovak Academy of Sciences, Dúbravská cesta 9, 845 07 Bratislava, Slovakia

The lanthanum substitution and sintering temperature variation effect on selected parameters of nickel-zinc ferrites were analyzed. To determine the structural parameters, we used X-ray diffraction together with SEM micrographs. The magnetic properties of ferrites were measured using thermomagnetic analysis methods and hysteresis loop measurements. Moreover, to analyze magnetic behavior of prepared polymer composites, we used the results of measuring the frequency dependences of the complex permeability. The ferrite filler content in all investigated composites was 60 vol.% and epoxy resin was used as the polymer matrix.

***Index Terms*—lanthanum-doped ferrites, polymer composites, structural properties, magnetic properties.**

I. Introduction

This work deals with the analysis of the results of selected types of measurements, which can be used to determine the structural and magnetic properties of lanthanum substituted nickel-zinc ferrites with spinel structure. These are soft magnetic materials that have extensive use in various applications due to their suitable properties including high saturation magnetization, high Curie temperature, high resistivity, low eddy current losses and relatively cheap production [1-3]. They are used in transformer cores, filters, power inductors, high-frequency components, etc [2,4]. In various applications, it is necessary to use different parameters of ferrites, which can be achieved in several ways. One of the ways to change the magnetic properties ferrites, is a change in the proportions of the starting materials during the production of the sample [5]. In our case, the ratio of nickel to zinc was the same for all the samples examined, namely 0.42:0.58. Only the lanthanum content was changed. As a trivalent element, it belongs to the group of rare earths and, when entering the crystal lattice, occupies the positions of trivalent iron ions. Rare earths including lanthanum play an important role in influencing magnetic properties such as electrical resistance and power losses [2]. They also play an important role in determining magnetic anisotropy [6]. We varied the lanthanum content for values x = 0, 0.02, 0.04, 0.06, 0.08 and 0.1, which appear in the formula $Ni_{0.48}Zn_{0.52}La_xFe_{2-x}O_4$. The next options that affect the properties of ferrites are the methods of sample production, different sintering temperatures and also the sintering time [7]. Our samples were produced by glycine-nitrate process based on auto-combustion preparation method, allowing the preparation of nanoparticles with small crystallite size variation together with high compositional homogeneity [8,9], and subsequently sintered at different temperatures (T = 400, 550, 700, 850, 1000, 1100, 1200, 1300°C), all for 6 hours. One sample was not sintered at all and is therefore a sample after decomposition. In addition, the authors supplemented the systematic influence of lanthanum substitution and sintering temperature on the investigated properties with an analysis of the magnetic behavior of selected nanoparticles used as fillers in polymer composites. These find application, among others, in the field of electromagnetic compatibility and/or microwave absorbers [10].

Manuscript received April 1, 2015; revised May 15, 2015 and June 1, 2015; accepted July 1, 2015. Date of publication July 10, 2015; date of current version July 31, 2015.
Corresponding author: M. Šoka (e-mail: martin.soka@stuba.sk).
Color versions of one or more of the figures in this paper are available online at http://ieeexplore.ieee.org.
Digital Object Identifier (inserted by IEEE).

II. Experiments and Results

A. Materials and Methods

A description of the chemical preparation of the samples and the measuring equipment used to determine the structural and magnetic properties of the samples were published in our previous article dedicated to a similar composition of samples, but sintered at only one temperature [11].

B. X-ray Diffraction

XRD diffraction patterns measured on powder samples of $Ni_{0.48}Zn_{0.52}Fe_2O_4$ and $Ni_{0.48}Zn_{0.52}La_{0.1}Fe_{1.9}O_4$ ferrites are shown in Fig. 1. Phase analysis confirmed a single-phase cubic spinel structure for all samples. Except for the lanthanum-substituted samples sintered at temperatures of 850 and 1000°C, the minor phase is designated as orthoferrite with a perovskite structure. At a higher sintering temperature, due to the redistribution of ions [12], this minor phase is incorporated into the spinel phase of ferrite. At a sintering temperature of 400°C and in the sample after decomposition, crystals do not yet begin to form and therefore we observe lower peaks. Table I shows the lattice constants and crystallite sizes. Lattice constants tend to decrease slightly with increasing sintering temperature, while substituted samples generally have higher ones, which may be due to the larger ionic radius of lanthanum ions compared to iron ions [13]. However, this is not the case for samples sintered at 850 and 1000°C, which is probably due to the formation of a secondary orthoferrite phase [14]. The size of the crystallites is significantly affected by the sintering temperature and the presence of lanthanum in the sample. It is true that the higher the sintering temperature, the larger the crystallite size. This means that increasing sintering temperature promotes their

growth [15], which is consistent with the increasing sharpness, or rather the size, of the peaks in Fig. 1. The measurement results further show that unsubstituted samples have larger crystallite size values, as the presence of lanthanum ions prevents their growth [16].

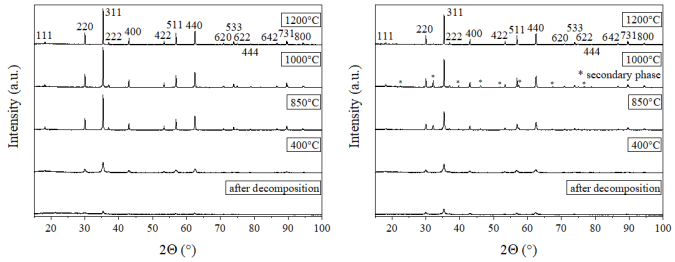

(a) (b)

Fig. 1. XRD patterns of (a) $Ni_{0.48}Zn_{0.52}Fe_2O_4$ and (b) $Ni_{0.48}Zn_{0.52}La_{0.1}Fe_{1.9}O_4$.

TABLE I. Lattice Parameters of $Ni_{0.42}Zn_{0.58}La_xFe_{2-x}O_4$

Sintering temperature (°C) / substitution amount *x*	Lattice parameter (Å)	Crystallite size (nm)
after decomposition / 0.00	8.41220 ± 0.0009	24.0 ± 1
400 /0.00	8.40600 ± 0.0003	21.6 ± 0.2
850 /0.00	8.40467 ± 0.00007	129 ± 2
1000 /0.00	8.40412 ± 0.00006	171 ± 3
1200 /0.00	8.40293 ± 0.00005	484 ± 21
after decomposition / 0.10	8.41380 ± 0.0005	17.6 ± 0.3
400 /0.10	8.41260 ± 0.0003	17.9 ± 0.2
850 /0.10	8.40200 ± 0.0001	50.4 ± 0.6
1000 /0.10	8.40264 ± 0.00008	134 ± 2
1200 /0.10	8.40300 ± 0.00008	336 ± 16

C. SEM micrographs

SEM micrographs of $Ni_{0.42}Zn_{0.58}La_{0.02}Fe_{1.98}O_4$ sintered at different temperatures are shown in Fig. 2. At 400°C, no particles are observable. Crystallization processes are not yet visible, which is also confirmed by the slightly sharp peaks on the diffractograms, although they are sharper than in the case of a sample after decomposition, which is still amorphous. At 850°C, small particles are already visible, which, although they do not crystallize yet, are the seeds of future crystals and are clearly separated from the volume of the amorphous mass of the sample. This trend continues when the temperature is increased to 1000°C, where the particles are already in the entire volume and begin to form cubic crystals. With a further increase in temperature, they grow and gradually crystallize in the entire volume.

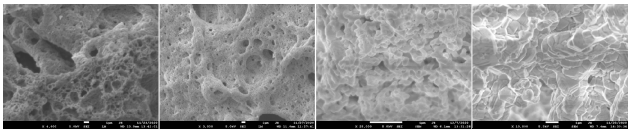

(a) (b) (c) (d)

Fig. 2. SEM micrographs of $Ni_{0.42}Zn_{0.58}La_{0.02}Fe_{1.98}O_4$ sintered at (a) 400, (b) 850, (c) 1000 and (d) 1200°C.

D. Thermomagnetic analysis

The temperature dependences of magnetic susceptibility provide useful information about the thermal stability and phase composition of the samples, see Fig. 3. At 400 and 550°C, the addition of lanthanum significantly affects their steepness, but this behavior disappears with increasing temperature. This can be explained by the fact that at lower temperatures, lanthanum is not sufficiently incorporated into the ferrite structure and thus its paramagnetic behavior prevails and weakens the magnetic susceptibility of the sample. At 550°C, the first Hopkinson peak appeared in the sample without lanthanum. It is characterized by a sharp increase in susceptibility with increasing temperature, showing a significant maximum below the Curie temperature. This phenomenon has to do with the movement of domain walls during the transition from a region with stable magnetization to a superparamagnetic state. [17]. As the sintering temperature increases, the number of Hopkinson peaks also increases. At 700°C, we can see three more significant peaks, and only traces of them are visible on the remaining three curves. For the sample without lanthanum content, thermomagnetic analysis indicates that there is a small amount of the second phase, due to a not so steep drop in magnetic susceptibility. At 850 and 1000°C, we observe Hopkinson peaks in all curves. At 850°C, they are significantly wider than at 1000°C. The steepest is with a lanthanum content of 0.06 at 850°C, and at 1000°C, it increased the most at a lanthanum content of 0.02, and the sample with a lanthanum content of 0.04 is close behind. From 1100°C, the Hopkinson peaks significantly decrease, but they are still observed in all samples. The decrease is a consequence of the higher magnetization of the samples, which is stable up to approximately 150°C for all materials. At 1200°C, almost all curves are without a Hopkinson peak, its small signs are visible only for samples with the highest two lanthanum contents. At 1300°C, the shape of all curves is not too steep, from which we can assume that a secondary phase occurs in all samples. The Hopkinson peak did not appear in any of them. From the comparison of the values of magnetic susceptibility at room temperature for all samples, a trend of increasing their values with the sintering temperature can be observed. This is probably related to the different magnetic arrangement due to the presence of lanthanum ions in the spinel matrix and to changes in the anisotropy of the demagnetizing field associated with the change in crystallites size [11].

E. Magnetic hysteresis loop measurement

Fig. 4a shows the hysteresis loops of ferrite $Ni_{0.42}Zn_{0.58}La_xFe_{2-x}O_4$ sintered at 1200°C. It is clear that with increasing La content the coercive field increases and thus the area of the hysteresis loop. The material tends to become magnetically harder. The substitution effect of lanthanum ions on the coercivity and permeability values $\mu_r@H_c$ is an interplay of several factors, such as the change in crystallite size, changes in magnetocrystalline anisotropy, or the presence of an orthoferrite phase at grain boundaries, which act as pinning centres for domain walls during the magnetization process [11]. This is also confirmed by the dependence of the differential relative permeability in the coercive field $\mu_r@H_c$,

which describes the mobility of the domain walls (Fig. 4b). At the point of the coercive field, domain walls moving processes are absolutely dominant. Compared to the state without substitution ($x = 0.00$), it decreased from the value of 631.4 to the value of 405.0 at maximum substitution ($x = 0.10$). The increase in the coercive field is also associated with the increase in the volume loss density during magnetization W from the value of 136.9 ($x = 0.00$) to the value of 289.2 ($x = 0.10$).

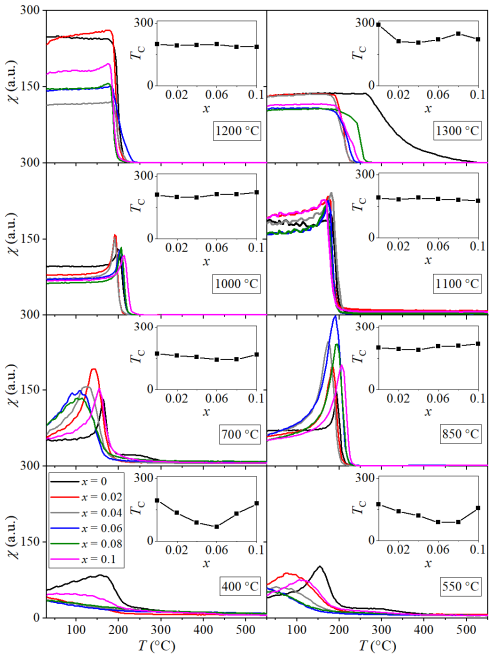

Fig. 3. Magnetic susceptibility temperature dependences and Curie temperatures of $Ni_{0.48}Zn_{0.52}La_xFe_{2-x}O_4$ sintered at different temperatures.

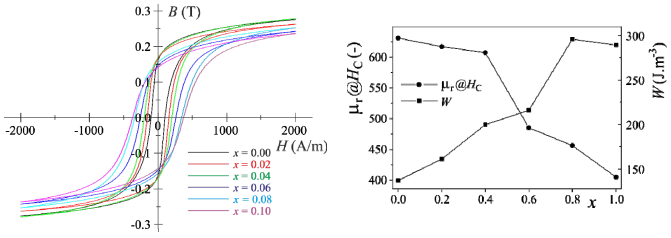

(a) (b)

Fig. 4. (a) Hysteresis loops of ferrite $Ni_{0.42}Zn_{0.58}La_xFe_{2-x}O_4$ sintered at 1200°C. (b) Selected parameters of ferrite $Ni_{0.42}Zn_{0.58}La_xFe_{2-x}O_4$ sintered at 1200°C.

F. Complex permeability spectra

The dependences of real μ′ and imaginary μ″ parts of complex (relative) permeability $\mu = \mu' - j\mu''$ of composites may be found in the Fig. 5. The composites have been fabricated from sintered ferrites $Ni_{0.42}Zn_{0.58}La_xFe_{2-x}O_4$ (x varied from 0.00 to 0.10 in steps of 0.02) used as a magnetic filler and epoxy resin used as a non-magnetic matrix. The particle size distribution (0-250 μm) and content (60 vol%) of filler particles in composite samples was constant. The ferrites were synthesized by two different methods: ceramic process (CP) at 1200°C for 6h and glycine nitrate process (GNP) at 1200°C and/or 1300°C for 6h, respectively. Selected structural and magnetic properties of sintered ferrites used as filler in composites can be found in Table II. Table III shows the substitution amount x of magnetic filler, preparation technology of filler, sintering temperature of filler, μ' of composites at $f = 1$ MHz, resonance frequency f_{res} of composites (at which the imaginary part μ'' has a peak). The permeability dependences portrayed in Fig. 5 attained similar treatment: below $f = 10$ MHz the μ' keeps almost constant, then over 10 MHz it starts to fall; simultaneously the μ'' grows at first and then declines. This is a relaxation type of permeability dispersion often observed in composite structures and is brought about the different magnetization mechanisms (namely the domain wall shifting and spin turning), [11,18].

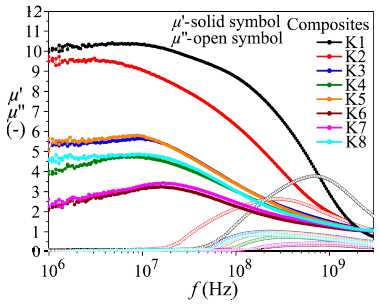

Fig. 5. Complex permeability spectra of composites.

TABLE II. Selected parameters of sintered ferrites $Ni_{0.42}Zn_{0.58}La_xFe_{2-x}O_4$ used as a filler in composites and prepared by the GNP and/or CP method

Substitution amount x	Theoretical density (g.cm^{-3})	Bulk density (g.cm^{-3})	Saturation magnetization M_S (kA/m)	Porosity (%)
0.00	5.3278	4.13	297.46	22.48
0.02	5.3623	4.52	273.18	15.71
0.04	5.3963	4.77	278.61	11.61
0.06	5.4348	4.66	268.58	14.26
0.06[1]	5.3163	5.04	247.73	5.20
0.08	5.4689	4.89	274.61	10.57
0.10	5.5059	4.77	265.37	13.4
[1]Sample prepared by the CP method				

TABLE III. Properties of fabricated composites with different preparation technology and sintering temperature of filler

Sample / substitution amount x	Method of ferrite filler preparation	Sintering temperature of ferrite filler (°C)	μ' at $f = 1$ MHz	f_{res} (MHz)
K1 / 0.06	CP	1200	10.1	695
K2 / 0.00	GNP	1300	9.5	242
K3 / 0.10	GNP	1300	5.3	202
K4 / 0.00	GNP	1200	3.8	298
K5 / 0.02	GNP	1200	5.4	273
K6 / 0.04	GNP	1200	2.2	597
K7 / 0.06	GNP	1200	2.3	704
K8 / 0.10	GNP	1200	4.6	196

In the following, we describes the variation of permeability with frequency from the viewpoint of distinct impacts (such as

sintering temperature, preparation technology, and substitution amount x) on resulted behavior of manufactured composite materials.

Effect of sintering temperature

For samples K2 and K4 without lanthanum ($x = 0.00$), the μ' value reduced from 9.5 to 3.8, while the resonant frequency increased from 242 to 298 MHz. A similar trend is observed for samples K3 and K8, only the changes in permeability and resonant frequency are smaller. The influence of temperature can be explained as follows. At a higher sintering temperature (1300°C) the ferrite has a lower concentration of defects in crystal lattice, larger grains and less slowed domain walls, and therefore lower coercivity and higher permeability.

Effect of preparation technology

Sample K1 (produced by CP and with $x = 0.06$) has five times greater permeability and about three times higher resonant frequency than sample K7 (produced by GNP and with $x = 0.06$). With CP technology, a higher density and four times lower porosity of the final ferrite used as a filler in the composite were accomplished, and this had a direct impact on the reached permeability and resonant frequency values.

Effect of La content

For samples K4, K5, K6, K7 and K8 prepared by GNP technology at a temperature of 1200°C, a variation of the permeability and resonance frequency values is observed approximately in accordance with the variation of the ferrite density (used as a filler), porosity and calculated saturation magnetization (permeability is directly proportional to magnetization and inversely proportional to the coercivity or effective anisotropic field). On the one hand, a change in the amount of lanthanum directly affects mainly AB interaction (as a result of which the magnetization and coercivity change: the nonmagnetic La^{3+} ion replaces Fe^{3+} ion on B site which leads to the decrement of magnetization and increment of the coercivity) and on the other hand, the effective anisotropic field (or demagnetization field) decreases with increasing grain size and (primarily intergranular) porosity.

III. Conclusion

Analysis of the results of individual structural/magnetic characterization methods showed the influence of the sintering temperature and substitution of iron ions by lanthanum ions in the spinel structure on the investigated parameters. Thus, it is possible to prepare unique magnetic materials for specific applications by appropriately selected heat treatment and/or substitution of ions of the basic chemical composition by lanthanum ions.

Acknowledgment

This work was supported by the Scientific Grant Agency of the Slovak Republic (VEGA), under projects no. 1/0041/24 and 2/0099/2022. Special thanks to E. Dobročka for XRD.

References

[1] M.N. Akhtar and M.A. Khan, "Effect of rare earth doping on the structural and magnetic features of nanocrystalline spinel ferrites prepared via sol gel route," *J. Magn. Magn. Mater.*, vol. 460, pp. 268-277, Aug. 2018.

[2] N. Khatun, O. Goni, S. Islam, A.A. Shaikh, S.F.U. Farhad, Al-Mamun, S. Alam, N.I. Tanvir, S. Hossain, T. Paul and S. Islam, "Impact of lanthanum ions on structural, morphological, magnetic, optical and electrical properties of Cobalt-Zinc ferrites," *J. Magn. Magn. Mater.*, vol. 614, 172740, Feb. 2025.

[3] C. Chen, Q. Zhang, T. Yao and H. Wang, "Electrospinning synthesis of shuttle-shaped NiCuZn ferrites and effect of sintering temperature on their structural and magnetic properties," *Mater. Sci.*, vol. 57, pp. 11537-11545, Jun. 2022.

[4] M.A. Warsi, M. Hashim, M.I. Arshad, S. Alamri, A. Almohammedi and M.N. Akhtar, "Magnetodielectric, electrical, and physicochemical evaluations of rare earth La^{3+}doped spinel nano ferrites for microwave absorption applications," *Mater. Chem. Phys.*, vol. 341, 130889, Sep. 2025.

[5] M.N. Akhtar, M. Yousaf, Y. Lu, M.A. Khan, A. Sarosh, M. Arshad, M. Niamat, M. Farhan, A. Ahmad and M.U. Khallidoon, "Physical, structural, conductive and magneto-optical properties of rare earths (Yb, Gd) doped Ni–Zn spinel nanoferrites for data and energy storage devices," *Ceram. Int.*, vol. 47, pp. 11878-11886, May 2021.

[6] G. Katoch, G. Sharma, V. Jain, A. Rajiv, J. Tham, A. Singh, V. Kaushik, T. Kalyani, A. Bhowmik and J. Santhosh, "Impact of lanthanum doping on crystal structure and magnetic anisotropy of Mn-Zn soft nanoferrites," *Sci. Rep.*, vol. 15, 11663, Apr. 2025.

[7] P. Akhtar, M.N. Akhtar, M.A. Baqir, A. Ahmad, M.U. Khallidoon, M. Farhan and M.A. Khan, "Structural and magnetic evaluations of rare-earths (Tb, Pr, Ce, Gd, Y)-doped spinel ferrites for high frequency and switching applications," *J. Mater. Sci: Mater Electron*, vol. 32, pp. 7692-7703, Feb. 2021.

[8] G.R. Mirshekari, S.S. Daee, H. Mohseni, S. Torkian, M. Ghasemi, M. Ameriannejad, M. Hoseinizade, M. Pirnia, D. Pourjafar, M. Pourmahdavi and K. Gheisari, "Structure and magnetic properties of Mn-Zn ferrite synthesized by glycine-nitrate auto-combustion process," *Adv. Mater. Res.*, vol. 409, pp. 520-525, Nov. 2011.

[9] W. Sami, "Synthesis and study of temperature effect on the spectroscopic properties of the nickel ferrites by glycine-nitrate auto-combustion," *Bas. J. Sci.*, vol. 40, pp. 138-149, Jun. 2022.

[10] N.A.M. Alsaif, H. Al-Ghamdi, R.A. Elsad, M.S. Shams, M.A. El-Shorbagy, A.S. Abouhaswa, Y.S. Rammah and S.M. Shaaban, "PVC doped with $Ni_{0.5}Pb_{0.5}Fe_2O_4$ spinel ferrites nanoparticles: Fabrication, structural, optical, and radiation shielding properties," *Radiat. Phys. Chem.*, vol. 212, 111145, Nov. 2023.

[11] M. Šoka, M. Ušáková, R. Dosoudil, E. Ušák and J. Lokaj, "Effect of lanthanum substitution on structural and magnetic properties of nickel zinc ferrites," *AIP Adv.*, vol. 8, 047802, Apr. 2018.

[12] S.K. Jakkaraju, K.V. Kumar and N.H. Kumar, "Influence of calcination temperature on gadolinium doped magnesium-zinc ferrite nanoparticles: Structural, optical, and photocatalytic properties for water splitting applications," *Next Mater.*, vol. 8, 100705, Jul. 2025.

[13] G. Katoch, G. Sharma, V. Jain, A. Rajiv, J. Tham, A. Singh, V. Kaushik, T. Kalyani, A. Bhowmik and J. Santhosh, "Impact of lanthanum doping on crystal structure and magnetic anisotropy of Mn-Zn soft nanoferrites," *Sci. Rep.*, vol. 15, 11663, Apr. 2025.

[14] Y.K. Dasan, B.H. Guan, M.H. Zahari and L.K. Chuan, "Influence of La^{3+} substitution on structure, morphology and magnetic properties of nanocrystalline Ni-Zn ferrite," *PLoS One*, vol. 12, e0170075, Jan. 2017.

[15] P.Thakur, R. Sharma, V. Sharma and P. Sharma, "Structural and optical properties of $Mn_{0.5}Zn_{0.5}Fe_2O_4$ nano ferrites: effect of sintering temperature," *Mater. Chem. Phys.*, vol. 193, pp. 285-289, Jun. 2017.

[16] Zulhadjri, N. Pratiwi, Y.E. Putri, Rahmayeni, N. Mufti, Ramli, V. Saraswaty and S. Sufian, "La^{3+} doped $ZnFe_2O_4$ synthesized via green chemistry approach using *Uncaria gambir Roxb*: A study on structural, optical, magnetic, and photocatalytic properties," *J. Photochem. Photobiol. A: Chem.*, vol. 461, 116168, Apr. 2025.

[17] M. Šoka, M. Ušáková, R. Dosoudil, V. Jančárik, E. Ušák and E. Dobročka, "Ni/Zn ratio and La substitution effect on selected structural and magnetic properties of NiZn ferrites," *J. Phys.: Condens. Matter*, vol. 36, 265801, Apr. 2024.

[18] R. Dosoudil, M. Ušáková, A. Grusková and J. Sláma, "Influence of the synthesis method of filler on permeability and microwave absorption properties of ferrite/polymer composites," *IEEE Trans. Magn.*, vol. 50, 2800204, Apr. 2014.